Kinetic Theory and Fast Wind Observations of the Electron Strahl

Konstantinos Horaites[1], Stanislav Boldyrev[1,2], Lynn B. Wilson III[3], Adolfo F. Viñas[3], Jan Merka[3,4]

[1]University of Wisconsin-Madison, [2]Space Sciences Institute, [3]NASA Goddard Space Flight Center, [4]Goddard Planetary Heliophysics Institute

Abstract

The solar wind strahl is a narrow, field-aligned population of high-energy electrons that originate in the solar corona. The beam-like shape of the strahl in velocity space is believed to come from the competition of two physical processes: the mirror force tends to narrow this population, while Coulomb collisions and wave-particle interactions tend to broaden it. Using data from the Wind satellites's SWE strahl detector, we investigate the detailed shape of the strahl and compare with predictions from a kinetic scale-invariant model.

Kinetic Equation

Let us assume the solar wind density, temperature, and magnetic field strength vary as power laws with the linear distance x along a flux tube:

$$n(x) \propto x^{\alpha_n}, T(x) \propto x^{\alpha_T}, B(x) \propto x^{\alpha_B} \quad (1)$$

We here characterize the electron strahl in the solar wind in terms of a scale-invariant kinetic theory. From this point of view the Knudsen number γ, which characterizes the importance of Coulomb collisions, is the central parameter that determines the shape of the distribution function $f(x, \mathbf{v})$. The self-similar kinetic equation is the drift-kinetic equation written under a change of variables (see "Definitions" below), with the condition $\gamma(x) \propto x^{\alpha_\gamma}$. In the high energy ($\xi >> 1$), field-aligned ($\mu \approx 1$) regime, the kinetic equation can be written as (ref. [1]):

$$\alpha F + \xi\frac{\partial F}{\partial \xi} + (2 - \alpha_\gamma/\alpha_T - \alpha')(1-\mu)\frac{\partial F}{\partial \mu} = \frac{\beta}{\gamma(x)\xi^2}\frac{\partial}{\partial \mu}(1-\mu)\frac{\partial F}{\partial \mu}. \quad (2)$$

Where we used the definitions:

$$f(\mathbf{v}, x) = \frac{NF(\mathbf{v}/v_{th}(x), x)}{T(x)^\alpha}, \gamma(x) \equiv -\frac{T^2(d\ln T/dx)}{2\pi e^4 \Lambda n}$$

$$\mu \equiv \mathbf{v}\cdot\mathbf{B}/(|v||B|) = \cos\theta, \xi \equiv \left(\frac{v}{v_{th}}\right)^2$$

$$\beta \equiv (1+Z_{eff})/2, \alpha' \equiv 2 - \alpha_\gamma/\alpha_T - (\alpha+1/2)\alpha_B, \quad (3)$$

Asymptotic Solution

Equation 2 has solutions for the distribution $F(x,\xi,\mu)$ of the form:

$$F(x,\xi,\mu) \sim (x/x_0)^{\alpha_s}\xi^\epsilon \exp\left\{\tilde{\gamma}(x)\Omega\xi^2(1-\mu)\right\} \quad (4)$$

Where we introduced $\Omega \equiv -\alpha'\alpha_T/\beta$, $\tilde{\gamma} \equiv \gamma/|\alpha_T|$. The full width at half maximum, θ_{FWHM}, is given by:

$$\theta_{FWHM} \approx \frac{2}{\xi}\sqrt{\frac{2\ln(1/2)}{\tilde{\gamma}\Omega}}. \quad (5)$$

Data—SWE Strahl Detector

Our data comes from the Wind satellite's SWE strahl detector [2], a high resolution electrostatic analyzer.

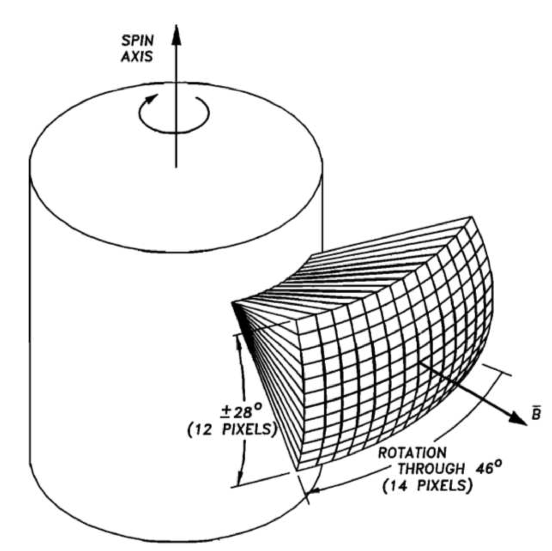

Figure: The SWE strahl detector measured electron counts in a 14x12 angular grid centered on the $\mathbf{B}$ field, as above (from [2]).

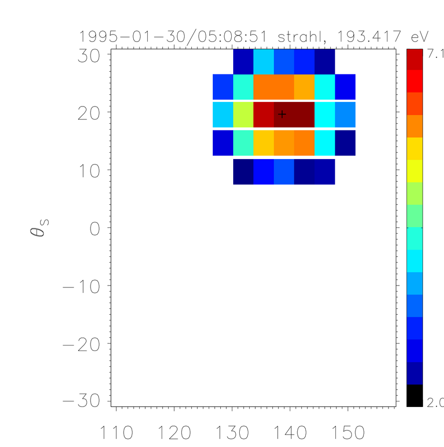

Figure: An angular distribution measured by the SWE strahl detector. The strahl (shown) is isolated from the background.

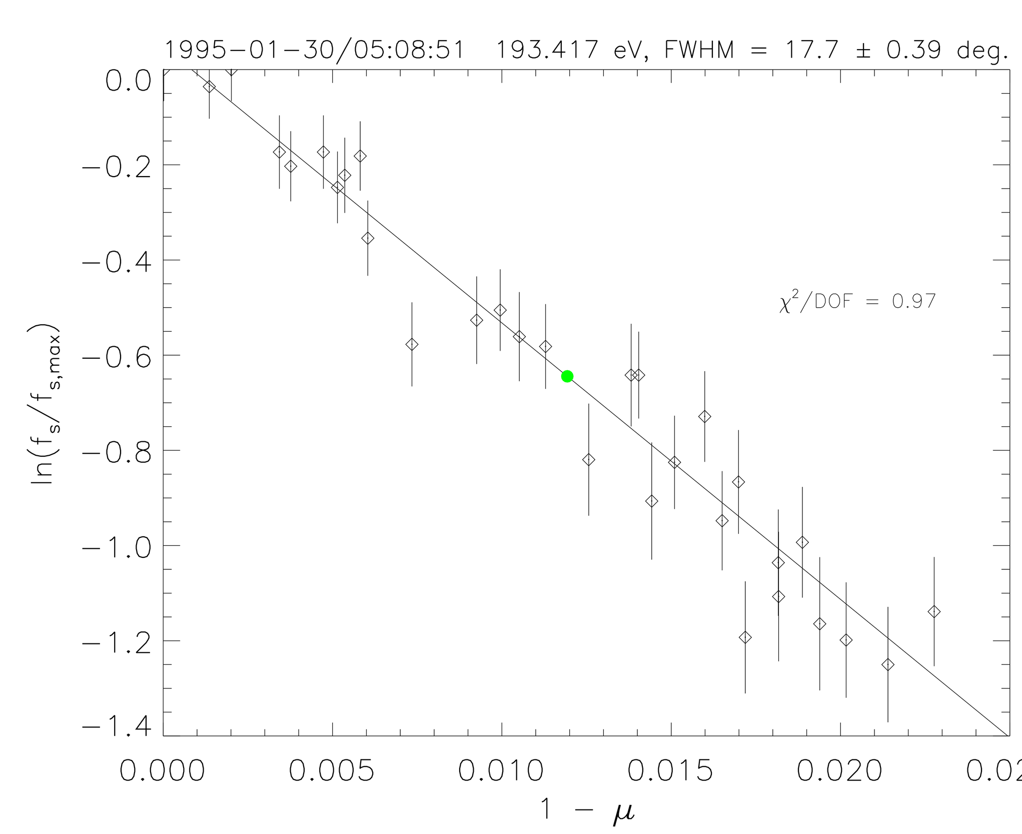

Figure: The full width at half-maximum, θ_{FWHM}, of the strahl (green) at constant energy is found by fitting the data in the vicinity of the strahl peak to the function $y = mx$, where $x = (1-\mu)$ and $y = \ln(F/F_{peak})$.

Results

Our linear fitting procedure for the slope m is equivalent to measuring the quantity Ω for each pitch angle distribution (PAD). Explicitly, $\Omega = m/(\tilde{\gamma}\xi^2)$. We set $\Omega = -0.34$, which is the average value inferred from our measurements, to calculate an "Expected θ_{FWHM}" for each PAD. We then compare with the "Measured θ_{FWHM}" calculated from the fitting procedure.

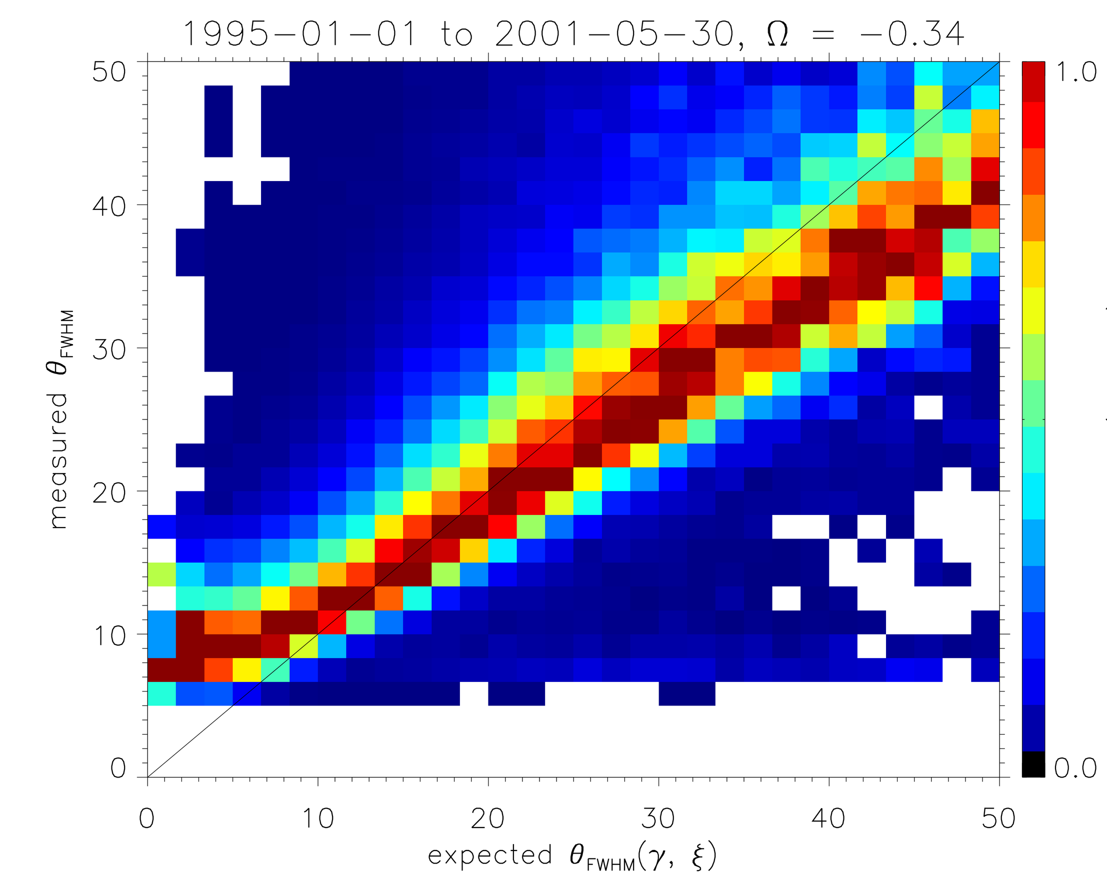

Figure: Expected strahl widths (FWHM, in degrees) from equation 4, plotted versus measured widths. The parameter Ω determines the slope of the data above. Setting $\Omega = -0.34$ shows very good agreement between our model and the data.

From equation 5, we obtain the following scaling relations for fixed x and Ω:

i For given n, $\theta_{FWHM} \propto \mathcal{E}^{-1}$

ii For given $\mathcal{E}$, $\theta_{FWHM} \propto \sqrt{n}$

These relations show how the strahl width varies with density n and energy $\mathcal{E}$, and are verified below.

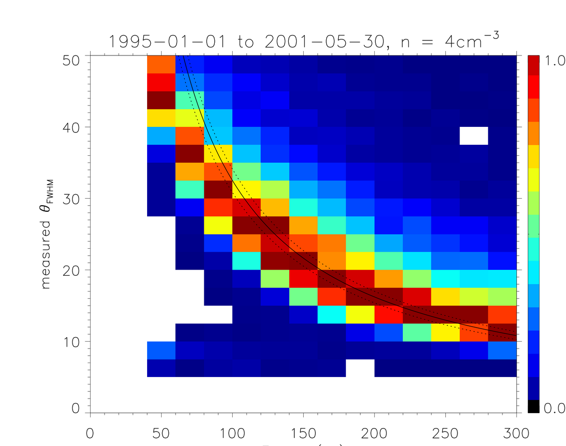

Figure: Verification of scaling relation (i): $\theta_{FWHM} \propto \mathcal{E}^{-1}$. Data shown in histogram fall in density range $3.6 < n < 4.4$ cm^{-3}.

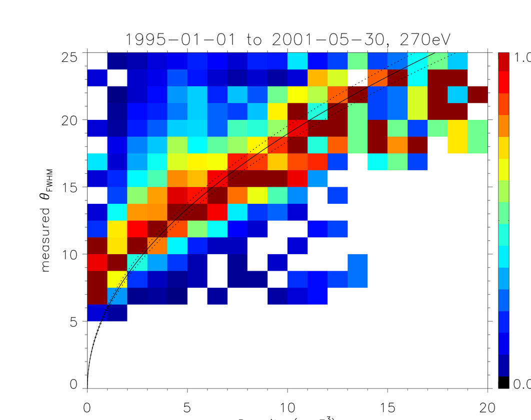

Figure: Verification of scaling relation (ii): $\theta_{FWHM} \propto \sqrt{n}$. Data shown in histogram measured at energy $\mathcal{E} = 270$ eV.

Fitting to F_{ave}

Although the SWE strahl detector sampled the eVDF one energy (ξ) at a time, these angular distributions can be averaged together to construct an average eVDF, F_{ave}.

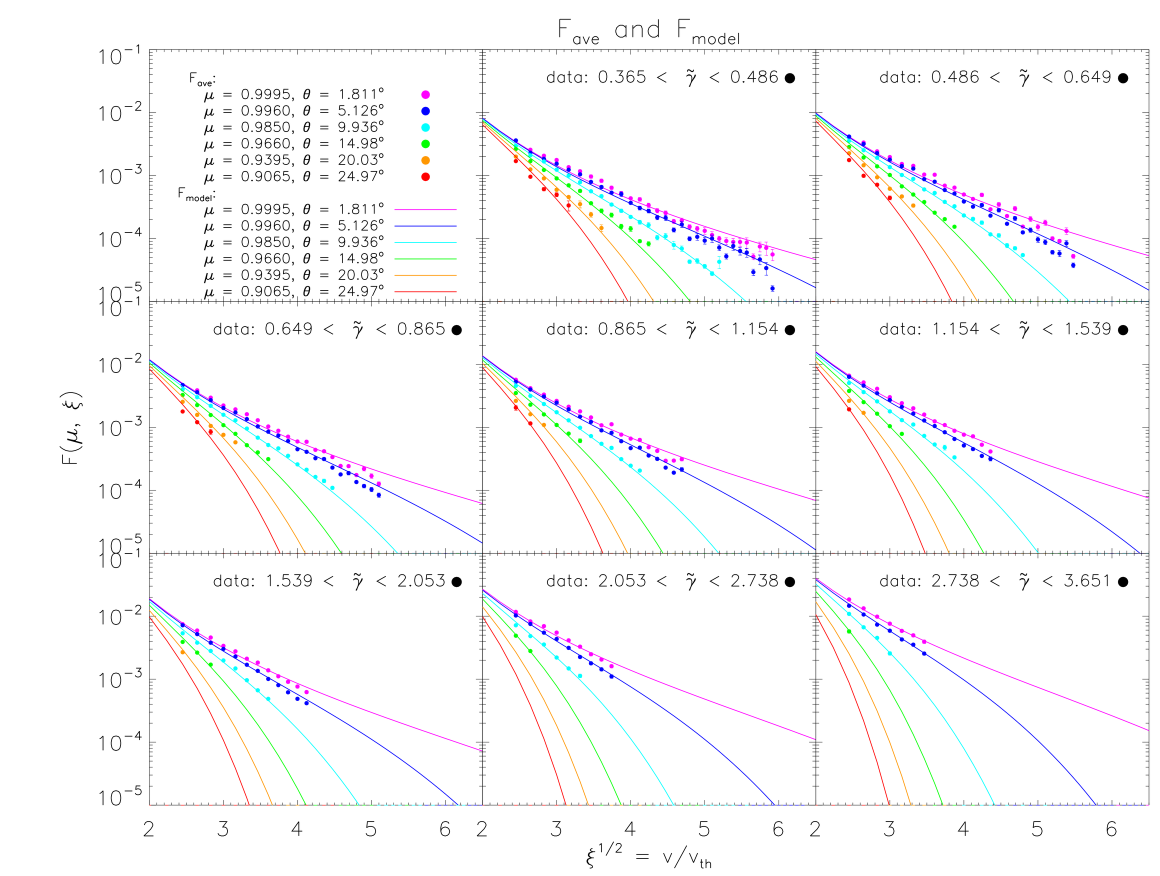

Figure: The average eVDF, F_{ave}, shown for various Knudsen numbers. Fits to eq. 4 are shown as lines.

Conclusions

- The asymptotic solution (4) accurately describes the shape of the strahl distribution.

References

[1] K. Horaites, S. Boldyrev, L. B. Wilson, III, A. F. Viñas, and J. Merka.
Kinetic Theory and Fast Wind Observations of the Electron Strahl.
ArXiv e-prints, June 2017.

[2] K. W. Ogilvie, D. J. Chornay, R. J. Fritzenreiter, F. Hunsaker, J. Keller, J. Lobell, G. Miller, J. D. Scudder, E. C. Sittler, Jr., R. B. Torbert, D. Bodet, G. Needell, A. J. Lazarus, J. T. Steinberg, J. H. Tappan, A. Mavretic, and E. Gergin.
SWE, A Comprehensive Plasma Instrument for the Wind Spacecraft.
, 71:55–77, February 1995.

Contact Information

- Website: http://home.physics.wisc.edu/~horaites/
- Email: horaites@wisc.edu